AGU PUBLICATIONS

JGR

Journal of Geophysical Research: Earth Surface

RESEARCH ARTICLE
10.1002/2013JF002823

Key Points:
- Connection of single-particle kinematics to particle velocity statistics
- Langevin equations based on the forces acting on a single particle
- Fokker-Planck equations for the PDF of particle velocities

Correspondence to:
E. Foufoula-Georgiou,
efi@umn.edu

Citation:
Fan, N., D. Zhong, B. Wu, E. Foufoula-Georgiou, and M. Guala (2014), A mechanistic-stochastic formulation of bed load particle motions: From individual particle forces to the Fokker-Planck equation under low transport rates, *J. Geophys. Res. Earth Surf.*, *119*, 464–482, doi:10.1002/2013JF002823.

Received 8 APR 2013
Accepted 19 JAN 2014
Accepted article online 25 JAN 2014
Published online 11 MAR 2014

A mechanistic-stochastic formulation of bed load particle motions: From individual particle forces to the Fokker-Planck equation under low transport rates

Niannian Fan[1,2], Deyu Zhong[1], Baosheng Wu[1], Efi Foufoula-Georgiou[2], and Michele Guala[2]

[1]State Key Laboratory of Hydroscience and Hydraulic Engineering, Tsinghua University, Beijing, China, [2]Department of Civil Engineering, Saint Anthony Falls Laboratory and National Center for Earth-Surface Dynamics, University of Minnesota, Minneapolis, Minnesota, USA

Abstract Bed load transport is a highly complex process. The probability density function (PDF) of particle velocities results from the local particle momentum variability in response to fluid drag and interactions with the bed. Starting from the forces exerted on a single particle under low transport rates (i.e., rolling and sliding regimes), we derive here the nonlinear stochastic Langevin equation (LE) to describe the dynamics of a single particle, accounting for both the deterministic and the stochastic components of such forces. Then, the Fokker-Planck equation (FPE), which describes the evolution of the PDF of the ensemble particle velocities, is derived from the LE. We show that the theoretical PDFs of both streamwise and cross-stream velocities obtained by solving the FPE under equilibrium conditions have exponential form (PDFs of both positive and negative velocities decay exponentially), consistent with the experimental data by Roseberry et al. (2012). Moreover, we theoretically show how the exponential-like PDF of an ensemble of particle velocities results from the forces exerted on a single particle. We also show that the simulated particle motions using the proposed Langevin model exhibit an emergent nonlinear relationship between hop distances and travel times (power law with exponent 5/3), in agreement with the experimental data, providing a statistical description of the particles' random motion in the context of a stochastic transport process. Finally, our study emphasizes that the motion of individual particles, described by the LE, and the behavior of the ensemble, described by the FPE, are connected within a statistical mechanics framework.

1. Introduction

Bed load is composed of those sediment particles that are rolling, sliding, or saltating along the riverbed, featured by frequent contact with the surface layer [*Einstein*, 1937; *Yalin*, 1977; *Van Rijn*, 1984; *Chien and Wan*, 1998]. Transport of bed load is the prevailing mode of sediment transport in gravel bed rivers or in coarse sand-bed rivers under low flow conditions [e.g., *Métivier et al.*, 2004; *Meunier et al.*, 2006; *Liu et al.*, 2008]. As a result, understanding and predicting bed load transport under various flow and boundary conditions have important implications for a broad range of research applications such as studying bed form evolution for stratigraphic interpretation, bank erosion, flood control, and stream restoration [e.g., *Bagnold*, 1977; *Yalin*, 1977; *Best*, 2005; *Church*, 2006].

Despite considerable research on bed load transport over the past several decades, the problem remains not well understood. One of the main challenges lies on the fact that motions of individual particles happen randomly, thus unveiling a highly complex stochastic process [e.g., *Papanicolaou et al.*, 2002; *Ancey et al.*, 2006; *Singh et al.*, 2009; *Foufoula-Georgiou and Stark*, 2010; *Martin et al.*, 2012; *Furbish et al.*, 2012a]. The stochasticity of particle motion as bed load results from the complex particle/fluid, particle/particle, and particle/boundary interactions. The first pioneering work focusing on the stochastic aspects of bed load transport can be tracked to *Einstein* [1937]. *Einstein* [1950] considered that a single particle moved in discrete hops and was interrupted by rest periods, and the statistical properties of hop distances and travel times were studied. Following the seminal work of *Einstein* [1937, 1950], several researchers have proposed stochastic formulations for studying bed load transport. For instance, the statistical properties of hop distances were studied from flume experiments [e.g., *Tsujimoto*, 1978; *Schmidt and Ergenzinger*, 1992; *Hu and Hui*, 1996; *Niño and García*, 1998a; *Wong et al.*, 2007; *Hill et al.*, 2010] or field observations [e.g., *Drake et al.*, 1988; *Hassan et al.*, 1991, 2013]. *Hunt* [1999] applied a probabilistic description borrowed from high-energy physics to study the entrainment of bed load particles, which

considered the stream as a reservoir of kinetic energy, analogous to heat baths. *Parker et al*. [2000] assigned a probabilistic structure not only to hop distance but also to entrainment and deposition and then proposed a generalized probabilistic Exner formulation. *Ganti et al*. [2010] noted that the hop distance distribution of bed load particles could be heavy tailed (the tail of the PDF following a power law) in certain cases and proposed an anomalous advection-diffusion model for bed load transport. *Bradley et al*. [2010] revisited a 50 year old tracer experiment in which the classical models performed poorly in predicting the tracer plume behavior; alternatively, they proposed a fractional advection-dispersion model and showed that the prediction by the new model fitted the experimental data quite well. *Ancey et al*. [2008] developed a framework based on a birth-death immigration-emigration Markov process to describe the particle exchanges between the bed and the water stream and showed how strong fluctuations in solid discharge could arise. Based on the framework described in *Ancey et al*. [2008], *Ancey* [2010] further proposed a stochastic form of the Exner equation and showed that such a model transformed into a Fokker-Planck representation in the large number limit.

As summarized above, it is noted that a growing number of methods borrowed from mathematics and physics are used to investigate bed load transport, especially its stochastic (or probabilistic) characteristics. However, most of the stochastic models are not physically based, at least at the particle scale, thus requiring some input from experimental observations.

Recent improvements in experimental techniques allow to sample particle trajectories at high spatial and temporal resolution. In particular, the experiments conducted by *Roseberry et al*. [2012] used high-speed imaging technology with 0.004 s temporal resolution to measure coarse sand particles transported as bed load over a plane bed consisting of erodible coarse sand particles without bed forms. The experimental results revealed important characteristics of both individual particle motions (microscale) and the collective behavior of these motions (macroscale). From the experimental data, *Roseberry et al*. [2012] showed that the probability density functions (PDFs) of both the streamwise and cross-stream particle velocities are exponential like (i.e., decay exponentially for both positive and negative velocities) and that the relationship between hop distances and the associated travel times is nonlinear. An independent experiment conducted by *Lajeunesse et al*. [2010] also showed the exponential-like PDFs of both the streamwise and cross-stream particle velocities. Aside from the field of bed load transport, it is noted that the exponential-like PDF of particle velocities has also been reported in the field of theoretical physics [*Touchette et al*., 2010; *Baule and Sollich*, 2012] and granular materials [*Murayama and Sano*, 1998; *Kawarada and Hayakawa*, 2004]. The presence of an exponential PDF in particle velocities by independent experiments indicates an emergent property of bed load particle motion calling for a theoretical and physical explanation.

Toward this goal, *Furbish et al*. [2012a] formulated a random walk model, resulting from the solution of their Fokker-Planck equation and informed by some key statistical properties of the particle velocity fluctuations observed in the experimental data of *Roseberry et al*. [2012]. They showed that this model reproduces the exponential-like PDFs of both the streamwise and cross-stream particle velocities and also the nonlinear relationship between hop distances and travel times. More recently, *Furbish and Schmeeckle* [2013] used a probabilistic derivation analogous to the formulation leading to Maxwell-Boltzmann distribution and showed that under equilibrium state for a large number of particles, the probability of finding a physical system (or part of this system) in a given state defined by its momentum is given by the exponential function. However, both models (*Furbish et al*. [2012a] and *Furbish and Schmeeckle* [2013]) were formulated from a physically based statistical perspective without explicitly accounting for the mechanistic forces acting on individual particles, i.e., for the particle motion kinematics dictated by their interaction with the bed and the carrying fluid.

In this study, we propose such a mechanistic-stochastic formulation of particle motion in its simplest possible form. Specifically, we begin by analyzing the forces exerted on a single particle and we formulate a Langevin equation (LE), describing the evolution of a single particle's velocity, in both the streamwise and cross-stream directions. Then, the Fokker-Planck equation (FPE), describing the evolution of the PDF of particle velocities, is derived from the Langevin equation. It is shown that the PDFs obtained by solving the FPE under equilibrium conditions have exponential forms. We also simulate the velocity series of individual particles from the LE and show the nonlinear relationship between hop distances and travel times.

To the best of our knowledge, no study has proposed a mechanistically formulated Langevin equation as the starting point for deriving the Fokker-Planck equation to investigate bed load transport (see also the discussion in *Frey and Church* [2011]). We hope that our development sheds light in this direction and provides further impetus

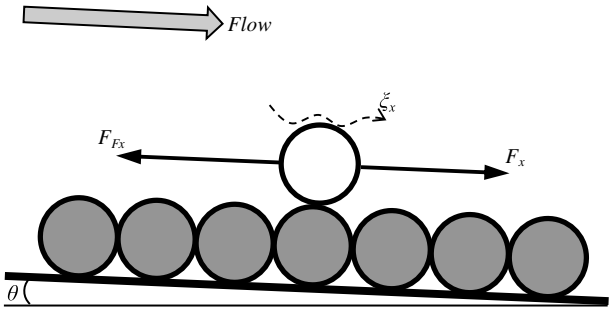

Figure 1. Schematic diagram of forces exerted on a single particle in the streamwise direction for rolling and sliding regimes: the friction force F_{Fx}, the constant mean downstream force F_x, and the stochastic part ξ_x. The friction force F_{Fx} has the form $F_{Fx} = -\Delta_x \cdot \mathrm{sign}(u_p)$, indicating that the magnitude is constant but the direction is opposite to that of particle velocity; the stochastic part ξ_x has zero mean and variance $\langle \xi_x(t_1)\xi(t_2)\rangle = 2D_x\delta(t_2 - t_1)$.

for theoretical as well as experimental studies at the particle scale in a Lagrangian framework. The paper is structured as follows. In section 2, we present the derivation of the Langevin equation for a single-particle velocity and the Fokker-Planck equation for an ensemble of particles. In section 3 we compare the theoretical results to the experimental data of *Roseberry et al*. [2012]. In section 4 we discuss our results, including a further analysis of the parameters in our model, and in section 5 we present our conclusions. In the appendix, we describe in detail the derivation of the Fokker-Planck equation from the Langevin equation.

2. Model Development

2.1. The Langevin Equation for a Single-Particle Velocity

We consider a two-dimensional steady water stream flowing down a bed of slope θ, composed of cohesionless uniform spherical particles of consistent diameter d and density ρ_p.

The forces exerted on a single particle per unit mass in the streamwise direction illustrated in Figure 1 are (1) the downslope component of submerged weight $W \sin\theta$ (where W is submerged weight per unit mass), (2) the resistance frictional force F_{Fx} due to the contact between bed load particles and the immobile bed, and (3) the fluid drag force F_{Dx}. The lift force is not accounted for because its effect on particle movement was observed to be relatively negligible for rolling and sliding regimes [*Schmeeckle and Nelson*, 2003].

Here we apply a Coulomb-like friction, which can be expressed in terms of the dynamic friction coefficient and the perpendicular bed surface component of submerged weight of the particle as [*Bagnold*, 1966; *Bridge and Dominic*, 1984]

$$F_{Fx} = \mu W \cos\theta \tag{1}$$

where μ is the dynamic friction coefficient. Strictly speaking, the Coulomb-like friction is only appropriate for a sliding block on a plane [*Gabet and Mendoza*, 2012], and for granular materials with bumpy surface, μ is a function of velocity [*Batrouni et al*., 1996; *Ancey et al*., 2003]. However, it is also universally applied in the study of particle transport, and μ is assumed a constant [*Bridge and Bennett*, 1992; *Parker et al*., 2003; *Abrahams and Gao*, 2006].

So in this study for a particle in motion, the magnitude of friction is constant, but the direction is opposite to the direction of velocity. As a result, the friction force has the form

$$F_{Fx} = -\Delta_x \cdot \mathrm{sign}(u_p) \tag{2}$$

where $\Delta_x = \mu W \cos\theta$ is a shorthand notation, u_p is the particle velocity in the x direction, and $\mathrm{sign}(u_p)$ stands for the sign of u_p, with the convention $\mathrm{sign}(0) = 0$ [*Touchette et al*., 2010]

$$\mathrm{sign}(u_p) = \begin{cases} 1, & u_p > 0 \\ 0, & u_p = 0 \\ -1 & u_p < 0 \end{cases} \tag{3}$$

Based on the study of *Schmeeckle et al*. [2007] and the modification by *Tregnaghi et al*. [2012a], the actual force exerted by the fluid on a particle can be expressed as

$$F_{Dx} = \frac{1}{2}\rho_f C_D A_f u_r \left(u_r^2 + v_r^2 + w_r^2\right)^{0.5} + F_{\mathrm{Accx}} \tag{4}$$

where ρ_f is the density of fluid, C_D is the drag coefficient, A_f is the area of the particle exposed to the fluid, u_r, v_r, and w_r are relative velocities between particle and fluid in the streamwise (x), cross-stream (y), and normal-stream (z) directions, respectively, and F_{Accx} is the acceleration force (sometimes called inertia force), which is produced primarily by spatial pressure gradients and is usually difficult to estimate [*Tregnaghi et al*., 2012a]. The first term in equation (4) is not easy to estimate either, because of the temporal fluctuations of turbulent

flows, local grain arrangement, exposure, and sheltering effects [*Tregnaghi et al.*, 2012a], and even the value of C_D for bed load in boundary layers has not been fully clarified yet [*Lee and Balachandar*, 2012].

The kinematic behavior of each particle is unique, even under simple conditions such as steady unidirectional turbulent flow over a plane sediment bed of uniform grains, due to the fluctuation of the resultant force exerted on the particles. However, there is an average downstream force exerted by the fluid on the particle, which allows us to decompose F_{Dx} into two parts: the average downstream drag force $\overline{F_{Dx}}$ and the fluctuation part F'_{Dx}, because most of the time $u_p \ll \overline{u}_f$, so for simplicity we assume $\overline{F_{Dx}}$ is independent of u_p.

To the best of our knowledge, no existing experimental studies have measured the forces exerted on particles in motion as bed load. The experimental studies on stationary particles have shown that under the condition of high relative turbulence intensities, the fluctuating component of the drag force is Gaussian like, partly due to the inertia force F_{Accx} which is proportional to the fluid acceleration du_f/dt [*Hofland et al.*, 2005; *Hofland and Battjes*, 2006; *Schmeeckle et al.*, 2007]. The experimental studies by *Diplas et al.* [2008] noted that the durations of the fluctuating forces are very short (milliseconds or tens of milliseconds). If we estimate the response time of the particle as the ratio between the settling velocity (computed as in *Chien and Wan* [1998]) and the acceleration due to gravity [*Zhong et al.*, 2011], we obtain values on the order of 0.1 s, overestimating by at least 1 order of magnitude the time scale of the fluctuating forces observed by *Diplas et al.* [2008]. Therefore, the effect of turbulence on the fluctuating drag F'_{D_x} is perceived by each particle as a sequence of short time scale perturbations and thus can be modeled as Gaussian white noise, as also proposed in the works of *Touchette et al.* [2010] and *Kawarada and Hayakawa* [2004].

Besides F_{Dx}, the friction force F_{Fx} is not steady either, and collisions between particles will also result in a fluctuating force; we treat all the fluctuating components of forces as Gaussian white noise ξ_x. We also take the average downstream drag force $\overline{F_{Dx}}$ and the downslope component of submerged weight $W \sin\theta$ together as a constant mean downstream force F_x. The forces exerted on a particle in the streamwise direction are sketched in Figure 1.

In addition, taking account of the friction force as expressed in equation (2), and by incorporating these three forces F_{Fx}, F_x, and ξ_x into Newton's second law, for a single particle per unit mass, we have

$$\frac{du_p}{dt} = -\Delta_x \cdot \mathrm{sign}(u_p) + F_x + \xi_x \tag{5}$$

where the Gaussian white noise ξ_x follows

$$\begin{aligned} \langle \xi_x(t) \rangle &= 0 \\ \langle \xi_x(t_1)\xi_x(t_2) \rangle &= 2D_x\delta(t_2 - t_1) \\ \langle \xi_x(t_1)\xi_x(t_2)\cdots\xi_x(t_{2n-1}) \rangle &= 0 \\ \langle \xi_x(t_1)\xi_x(t_2)\cdots\xi_x(t_{2n}) \rangle &= (2D_x)^n \sum [\delta(t_{i_1} - t_{i_2})\cdots\delta(t_{i_{2n-1}} - t_{i_{2n}})] \end{aligned} \tag{6}$$

where t is the time, δ is the Dirac delta function, n is a positive integer, and D_x denotes the amplitude of the fluctuating force (i.e., a measure of the variance of ξ_x).

Equation (5) is the Langevin equation (LE) which describes the evolution of u_p; the equation is a nonlinear stochastic differential equation, and "white noise" refers to the δ correlation property of ξ_x, which ensures the Markovian property of the process $u_p(t)$ [*Gardiner*, 1983; *Risken*, 1989; *Van Kampen*, 2010].

Similarly, we arrive at the Langevin equation describing the evolution of the particle velocity in the cross-stream direction v_p:

$$\frac{dv_p}{dt} = -\Delta_y \cdot \mathrm{sign}(v_p) + \xi_y \tag{7}$$

where the Gaussian white noise ξ_y follows

$$\begin{aligned} \langle \xi_y(t) \rangle &= 0 \\ \langle \xi_y(t_1)\xi(t_2) \rangle &= 2D_y\delta(t_2 - t_1) \\ \langle \xi_y(t_1)\xi_y(t_2)\cdots\xi_y(t_{2n-1}) \rangle &= 0 \\ \langle \xi_y(t_1)\xi_y(t_2)\cdots\xi_y(t_{2n}) \rangle &= (2D_y)^n \sum [\delta(t_{i_1} - t_{i_2})\cdots\delta(t_{i_{2n-1}} - t_{i_{2n}})] \end{aligned} \tag{8}$$

where D_y denotes the amplitude of ξ_y. Equation (7) is a simpler form than equation (5) because the average force in the cross-stream direction is zero.

Many researchers have developed theoretical models for the motion of sediment particles in turbulent flow and tried to calculate the forces exerted on particles accurately [e.g., *Wiberg and Smith*, 1985, 1989; *Niño and García*, 1998b; *Reynolds and Cohen*, 2002; *Schmeeckle and Nelson*, 2003; *Minier et al*., 2004; *Yeganeh-Bakhtiary et al*., 2009; *Brouwers*, 2010]. Here we adopt a simplified approach in which the forces acting on a particle are split into a deterministic and a stochastic additive component. A similar treatment was also adopted in *Jerolmack and Mohrig* [2005], in which the fluctuation in instantaneous bed stress was treated as stochastic by adding a Gaussian white noise term, and therefore, a Langevin-like equation, although not acknowledged as such, was obtained. For a definition of the Langevin equation in this context, see Appendix A.

2.2. The Fokker-Planck Equation for the PDF of the Ensemble Particle Velocities

From the Langevin equation, which describes the evolution of a single-particle velocity, we can derive the Fokker-Planck equation which describes the PDF of the ensemble of particle velocities. The detailed derivation is shown in Appendix A. The Fokker-Planck equation (FPE) derived from equations (5) and (6) for the PDF of u_p is

$$\frac{\partial \rho_{u_p}}{\partial t} = -\frac{\partial}{\partial u_p}\left\{\left[F_x - \Delta_x \cdot \mathrm{sign}\left(u_p\right)\right]\rho_{u_p}\right\} + D_x \frac{\partial^2 \rho_{u_p}}{\partial {u_p}^2} \tag{9}$$

where ρ_{u_p} is the PDF of u_p for a large number of particles.

Similarly, from equations (7) and (8), we derive the FPE for the PDF of v_p

$$\frac{\partial \rho_{v_p}}{\partial t} = -\frac{\partial}{\partial v_p}\left[-\Delta_y \cdot \mathrm{sign}\left(v_p\right)\rho_{v_p}\right] + D_y \frac{\partial^2 \rho_{v_p}}{\partial {v_p}^2} \tag{10}$$

where ρ_{v_p} is the PDF of v_p for a large number of particles.

Under the equilibrium condition, i.e., $\partial \rho_{u_p}/\partial t = 0$, we have

$$\frac{\partial}{\partial u_p}\left\{\left[F_x - \Delta_x \cdot \mathrm{sign}\left(u_p\right)\right]\rho_{u_p} - D_x \frac{\partial \rho_{u_p}}{\partial u_p}\right\} = 0 \tag{11}$$

The term in $\{\cdot\}$ of equation (11) is referred to as the probability current [*Risken*, 1989]. For the natural boundary conditions $\rho_{u_p}(+\infty) = 0$, the probability current is zero [*Risken*, 1989], so we have

$$\left[F_x - \Delta_x \cdot \mathrm{sign}\left(u_p\right)\right]\rho_{u_p} - D_x \frac{\partial \rho_{u_p}}{\partial u_p} = 0 \tag{12}$$

By integrating equation (12), we obtain

$$\rho_{u_p}\left(u_p\right) = C \exp\left(\frac{-\Delta_x \left|u_p\right| + F_x u_p}{D_x}\right) \tag{13}$$

where C is the normalization constant (i.e., the integration of equation (13) with respect to u_p is unit), whose value can be determined as

$$C = \frac{{\Delta_x}^2 - {F_x}^2}{2\Delta_x D_x} \tag{14}$$

Following the above derivation, we obtain the solution of the FPE under the equilibrium condition

$$\rho_{u_p}\left(u_p\right) = \frac{{\Delta_x}^2 - {F_x}^2}{2\Delta_x D_x} \exp\left(\frac{-\Delta_x \left|u_p\right| + F_x u_p}{D_x}\right) \tag{15}$$

Equation (15) is the theoretical PDF of particle streamwise velocities under equilibrium condition showing an exponential-like distribution; note that even though both sides of the distribution (for $u_p < 0$ and $u_p > 0$) are exponential, they are asymmetric. If $F_x > 0$, more particles have positive velocities and vice versa. The values of the ratios Δ_x/D_x and F_x/D_x determine the shape of the PDF: the larger the value of Δ_x/D_x, the narrower the PDF is and the larger the value of F_x/D_x, the more asymmetric the PDF is.

Similarly, equation (10) can also be solved under the equilibrium condition as

$$\rho_{v_p}\left(v_p\right) = \frac{\Delta_y}{2D_y} \exp\left(\frac{-\Delta_y \left|v_p\right|}{D_y}\right) \tag{16}$$

Equation (16) is just a two-sided exponential distribution (also referred to as Laplace distribution), which is symmetrical about $v_p = 0$. The value of Δ_y/D_y determines the shape of the PDF, with increasing values of Δ_y/D_y implying a narrower distribution.

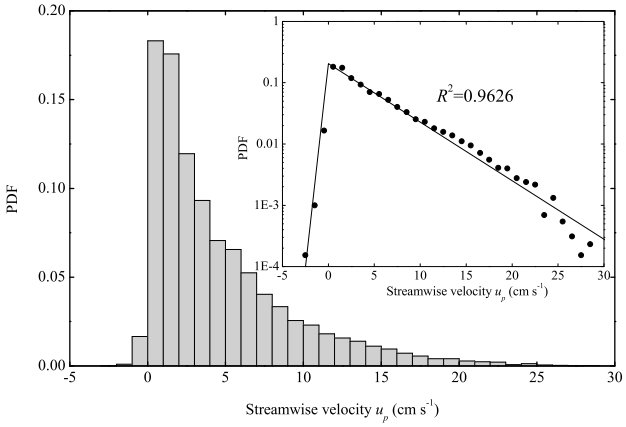

Figure 2. Empirical PDF of particle streamwise velocity u_p extracted from the experimental data by *Roseberry et al.* [2012]. The semilog plot (inset) shows both the empirical PDF of the experimental data (black dots) and the theoretical PDF (equation (15)) fitted to these data (solid line). Least squares regression gives the relation $\Delta_x/D_x = 1.64\ \mathrm{s \cdot cm^{-1}}$ and $F_x/D_x = 1.42\ \mathrm{s \cdot cm^{-1}}$.

Both equations (15) and (16) are exponential-like distributions; these theoretical distributions are consistent with the individual experimental data from *Lajeunesse et al.* [2010] and *Roseberry et al.* [2012].

3. Comparison With Experimental Data

3.1. Experimental Data

Roseberry et al. [2012] conducted a set of experiments within an 8.5 m × 0.3 m flume in the River Dynamics Laboratory of Arizona State University. The erodible bed was composed of relatively uniform sand with an average diameter of 0.5 mm. The Froude number F_r varied from 0.30 to 0.35, the Shields number τ_* varied from 0.034 to 0.063, and the particle Reynolds number Re_* ranged from 8.25 to 11.4, which indicated transitionally rough beds. The flow rate was low enough that no bed form was produced. The high-speed imaging of particle motions was 250 frames per second over durations ranging from 0.4 to 19.6 s. It was considered that a particle with $u_p = v_p = 0$ was at rest. Conversely, a particle was considered to be in motion if either u_p or v_p was finite, and then it was included in the statistical analysis.

The set of experiments comprises six runs (R1A, R2A, R3A, R5A, R2B, and R3B). For R3B, the temporal resolution was 0.004 s, and 12,944 paired velocity components (u_p and v_p) were involved, which was much more than the other experiments. As a result, we used the data from R3B, although in all runs the PDFs of streamwise and cross-stream velocities are exponential like [*Roseberry et al.*, 2012]. For more details about the experiments, see *Roseberry et al.* [2012].

3.2. PDF of Particle Velocities

We calibrate the theoretical PDFs provided by our model using the velocity data from R3B by *Roseberry et al.* [2012]. First, we compute the empirical PDF from the experimental streamwise velocity data, and then we compare it to the theoretical PDF described by equation (15) to obtain the following parameter relationships $\Delta_x/D_x = 1.64\ \mathrm{s \cdot cm^{-1}}$ and $F_x/D_x = 1.42\ \mathrm{s \cdot cm^{-1}}$ using least squares regression on semilog plot. Figure 2 shows the PDF of u_p from both the experimental data and the fitted theoretical curve proposed by our model. We note that the experimental data contain a small portion of negative u_p, which was neglected in the statistical analysis of *Furbish et al.* [2012a], and their random walk model could not produce negative velocities either. Our model is able to consider negative u_p, and the theoretical PDF agrees with the experimental data quite well for both positive u_p and negative u_p.

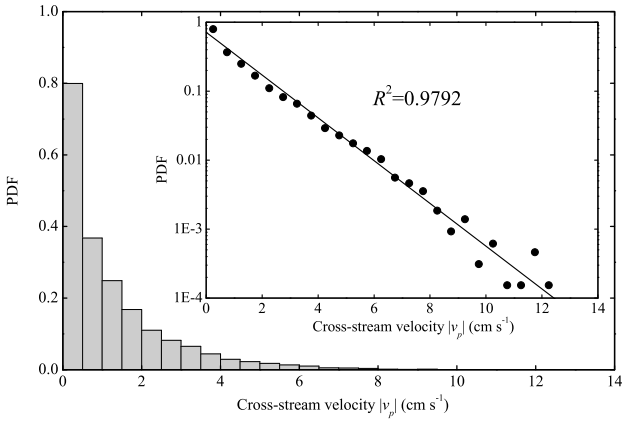

Figure 3. Empirical PDF of particle cross-stream velocity $|v_p|$ extracted from the experimental data by *Roseberry et al.* [2012]. The semilog plot (inset) shows both the empirical PDF of the experimental data (black dots) and the theoretical PDF, equation (16), fitted to these data (solid line). Least squares regression gives the relation $\Delta_y/D_y = 0.714\ \mathrm{s \cdot cm^{-1}}$.

We follow the same procedure for cross-stream velocities, computing the empirical PDF using the experimental data and then comparing it with the theoretical PDF described by equation (16) to obtain the

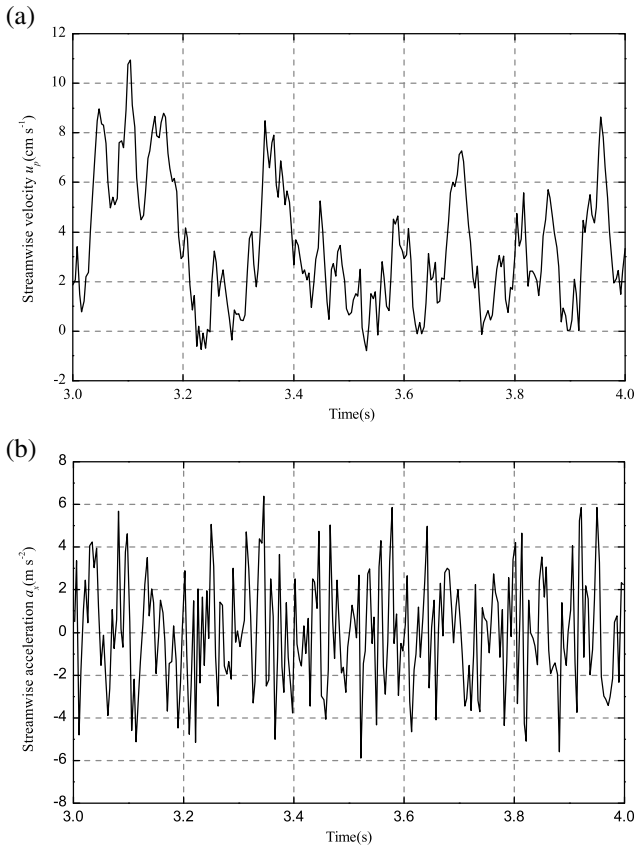

Figure 4. An example of simulated results for a single particle from 3.0 to 4.0 s by the numerical simulation of the Langevin equation (LE) (equation (17)). (a) The time series of streamwise velocity u_p. (b) The time series of streamwise acceleration a_x.

parameter ratio as $\Delta_y/D_y = 0.714\ \mathrm{s \cdot cm^{-1}}$. Because the distribution is symmetric, we only refer to the magnitude of the cross-stream velocity $|v_p|$. Figure 3 shows the PDF of $|v_p|$ from both the experimental data and our fitted theoretical model.

From the calibration of our model for the streamwise velocities, we obtained the values of the ratios Δ_x/D_x and F_x/D_x; therefore, by determining independently one of the three parameters Δ_x, F_x, and D_x, we can compute the remaining ones. Among them, Δ_x which can be expressed as $\Delta_x = \mu W \cos\theta$ is the easiest to determine, under the assumption that the variability of the local slope, at the grain scale, is negligible (implying a perfectly inclined bed, which is a reasonable assumption at low transport rates, with no bed forms and uniform grain size distribution). The value of the friction coefficient μ for particles moving in water has been studied intensively [e.g., *Bagnold*, 1966, 1973; *Hanes and Bowen*, 1985; *Bridge and Bennett*, 1992; *Abrahams*, 2003; *Abrahams and Gao*, 2006], and *Abrahams and Gao* [2006] noted that the value of μ could be taken as 0.6. Thus, given the water and sand particle densities of $\rho_f = 1000\ \mathrm{kg \cdot m^{-3}}$ and $\rho_p = 2650\ \mathrm{kg \cdot m^{-3}}$, respectively, and assuming the slope negligible (a valid assumption for the experiment of *Roseberry et al.* [2012]), i.e., implying $\cos\theta \to 1$, we obtain $\Delta_x = 3.66\ \mathrm{m \cdot s^{-2}}$. Considering the above obtained relationships $\Delta_x/D_x = 1.64\ \mathrm{s \cdot cm^{-1}}$ and $F_x/D_x = 1.42\ \mathrm{s \cdot cm^{-1}}$, we then compute the values $F_x = 3.17\ \mathrm{m \cdot s^{-2}}$ and $D_x = 0.0223\ \mathrm{m^2 \cdot s^{-3}}$ for the R3B of the experiment by *Roseberry et al.* [2012].

3.3. Numerical Simulation of the Langevin Equation

While the FPE solution provided in equation (15) gives the theoretical PDF of u_p, we need the LE described in equations (5) and (6) to get u_p for individual particles. We resort to a stochastic Runge-Kutta numerical algorithm, to discretize equations (5) and (6) as [*Zhang*, 2007]

$$\begin{aligned} F_1 &= -\Delta_x \cdot \mathrm{sign}\left[u_p(t) + w_1\sqrt{2D_x\Delta \mathrm{t}}\right] + F_x \\ F_2 &= -\Delta_x \cdot \mathrm{sign}\left[u_p(t) + \Delta \mathrm{t} \cdot F_1 + w_2\sqrt{2D_x\Delta \mathrm{t}}\right] + F_x \\ u_p(t+\Delta \mathrm{t}) &= u_p(t) + \frac{1}{2}(F_1 + F_2)\Delta \mathrm{t} + w_0\sqrt{2D_x\Delta \mathrm{t}} \end{aligned} \tag{17}$$

where F_1 and F_2 are Runge-Kutta coefficients, and w_0, w_1, w_2 are independent random numbers picked from a standard Gaussian distribution with zero mean and unit variance, which are created by the Box-Muller method [*Zhang*, 2007].

With the values of the parameters obtained before, i.e., $\Delta_x = 3.66\ \mathrm{m \cdot s^{-2}}$, $F_x = 3.17\ \mathrm{m \cdot s^{-2}}$, and $D_x = 0.0223\ \mathrm{m^2 \cdot s^{-3}}$, we simulated the series of u_p for 100,000 particles with zero initial u_p for all the particles. The time step used was $\Delta = 1 \times 10^{-4}$ s, while the temporal solution of the experiments was 4×10^{-3} s; as a result, we averaged every 40 values in our simulation, in order to match the time intervals of adjacent velocities of the experimental data. An

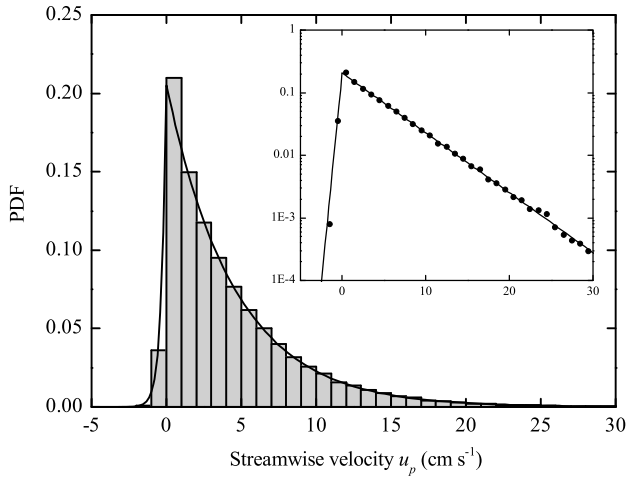

Figure 5. Empirical PDF of particle streamwise velocity u_p extracted from 100,000 numerically simulated particles (histogram) by the numerical simulation of the LE as equation (17) and the theoretical model (solid line) by the FPE as equation (15). The semilog plot (inset) highlights that the PDF is exponential like.

example of the simulated series of the streamwise velocity u_p and streamwise acceleration a_x of a single particle is shown in Figure 4. We extracted the PDF from these simulated u_p; the PDF was considered steady within a period t_s ($t_s \approx 0.8$ s). Figure 5 shows the PDF of u_p both extracted from the simulated data at the end of 2 s and the theoretical model provided by equation (15). As expected, the two PDFs are in good agreement, validating the numerical simulation of the particle motions described by the LE.

3.4. Accelerations of Particles

The particles entrain and stop, so the ensemble-averaged particle acceleration equals zero for steady state conditions [*Furbish et al.*, 2012a]. We study the acceleration of particles from the simulated velocities' series and verify that when the particles have reached the steady state conditions, the distribution of particle acceleration a_x is Gaussian with a zero mean value (Figure 6). For more details on the particle accelerations, see the discussion in section 4.1. We recall that our model derivation is relevant for low transport conditions where rolling and sliding (rather than saltating) grains dominate (see also discussion in section 4.1). Thus, we clarify that hop distance here refers to the travel distance between two consecutive stops ($u_p = 0$) and travel time to the time elapsed between these two consecutive stops.

3.5. Hop Distance and Travel Time

Under our model we can also study the hop distance λ and travel time τ. We use the stochastic Runge-Kutta algorithm described in equation (17) to simulate the movement of 100 particles for a duration of 0.4 s and assume that if the velocity falls below zero, the particle is disentrained; this treatment is similar to [*Furbish et al.*, 2012a] in the study of hop distances and travel times by their random walk model.

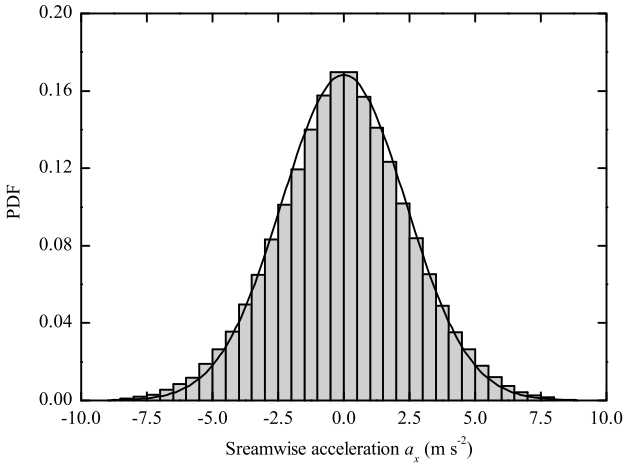

Figure 6. Empirical PDF of particle streamwise acceleration a_x extracted from 100,000 numerically simulated particles for steady state conditions and the fitted zero-mean Gaussian distribution shown as the solid line. The simulated distribution is qualitatively similar to that obtained from the statistical analysis of the experimental data by *Furbish et al.* [2012a] and an independent experimental study by *Ramesh et al.* [2011], but our figure is fuller because of the larger number of simulated data.

We compare our results to the experimental data by *Roseberry et al.* [2012] as shown in Figure 7; both show similar behavior and indicate the relation $\lambda \propto \tau^{5/3}$ as the solid line, which has also been shown by *Roseberry et al.* [2012] and *Furbish et al.* [2012a]. The results of our model (black circles) fit the experimental data (white circles) at least as well as the model by *Furbish et al.* [2012a] (see their Figure 17). Even though these results are obtained from one realization only and might differ somewhat among different realizations, one can observe that our model seems to slightly underestimate the hop distances for large travel times, while the opposite trend is observed in the model of *Furbish et al* [2012a] (compare our Figure 7 with their Figure 17). It is worth repeating here that, as is the case of the model of *Furbish et al.* [2012a], our model described by equation (17) does not know how λ and the associated τ relate to each other, as it only

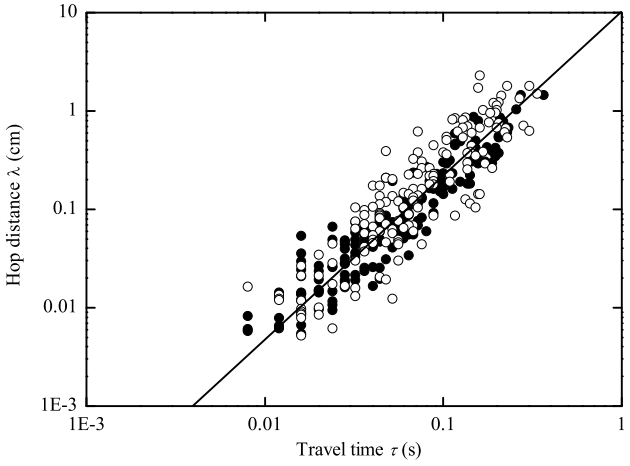

Figure 7. Plot of hop distance λ versus associated travel time τ shows the relation $\lambda \propto \tau^{5/3}$ (solid line); black circles are obtained from the model in this paper, involving 168 motions of 100 particles, and white circles are obtained from the experimental data of R3B by *Roseberry et al.* [2012], involving 153 motions of 100 particles. Hop distances smaller than 0.005 cm from both the experiment and the simulation are ignored.

considers the property of the forces exerted on particles; thus, the correct λ, τ relationship emerges from our model as a consequence of the prescribed particle dynamics.

4. Discussion

4.1. The Validity of Our Model

In the development of our model, the friction forces between the particles and the bed play an important role. As a result, our model is limited to low transport rate conditions where rolling and sliding are the dominant mode of the particles' motion. The experimental data analyzed here (R3B) were obtained with $\tau_* = 0.05$, thus below the threshold for saltation ($\tau_* < 0.1$) identified by *Hu and Guo* [2011]. As the bed shear stress increases, saltating replaces rolling and sliding and becomes the main regime of particles' motion [*Van Rijn*, 1984]. Another assumption embedded in our model is that only the particles on the top of the bed surface can move; this assumption becomes invalid under high transport rate conditions because a sheet consists of several layers of moving particles [*Hanes*, 1986; *Gao*, 2008].

Our model is thus developed for low transport rate conditions, e.g., the mean activity (number of moving particles per unit area) for R3B in *Roseberry et al.* [2012] is only 2.83 cm^{-2}, while the aerial density of particles is about 400 cm^{-2}. A large number of investigations also focused on low transport rate conditions [e.g., *Nikora et al.*, 2002; *Seminara et al.*, 2002; *Parker et al.*, 2003; *Francalanci and Solari*, 2007; *Wong et al.*, 2007; *Diplas et al.*, 2010; *Furbish et al.*, 2012c; *Martin et al.*, 2012], as sediment transport is such a complex process that it is almost impossible to develop a comprehensive framework focusing on all aspects of the problem [e.g., *Ancey et al.*, 2008].

Our model attempts to capture in the simplest possible form the dominant physical mechanisms of particle motion and is very parsimonious (three parameters). In addition to the ability to reproduce the exponential PDF of particle velocities and the nonlinear relationship between hop distances and travel times, the simulation results show that it can qualitatively reproduce the PDFs of particle displacements $q_u = u_p(t+\Delta) - u_p(t)$ conditioned on the streamwise particle velocity u_p (Figure 8) as suggested from the experimental data [*Furbish et al.*, 2012a, Figure 6]. Specifically, Figure 8 demonstrates that our model can reproduce the positive skewness of particle displacements for small velocities and the negative skewness for high velocities; however, it results in a range of velocity displacements which is narrower than that reported in *Furbish et al.* [2012a], especially for large velocities. We recall that our model has three parameters, out of which Δ_x was independently estimated as a function of the dynamic friction coefficient μ assumed to be equal to 0.6. If we relax this assumption and consider a larger value $\mu = 0.8$ (while maintaining the ratios Δ_x/D_x and F_x/D_x), the F_x and D_x parameters will be larger and the particle displacement PDFs will increase in their range (this was verified by simulation). Physically, this is justified in the sense that an increased friction coefficient will require a larger downstream force F_x and a larger variability in the stochastic component D_x in order to preserve the same distribution of particle velocities.

To provide more insight into the discrepancies between the observed PDFs of particle displacements and those produced by our model, we note that our model treats the fluctuating forces exerted on a single particle as a Gaussian white noise, with constant variance regardless of the height and velocity of the particle. While this assumption is consistent with near-bed physical processes (particle wall collisions, turbulent characteristic in the roughness sublayer), it may not be appropriate for the logarithmic and outer layers. Particles moving with a relatively high velocity are likely to be ejected out of the roughness sublayer and entrained by the large and very large scale turbulent structures that populate the logarithmic layer [e.g., *Guala et al.*, 2006, 2011; *Monty et al.*, 2007; *Keylock et al.*, 2013]. These structures are organized, spatiotemporally coherent, extending in the streamwise direction 6–10 times the outer scale (in this specific case, the

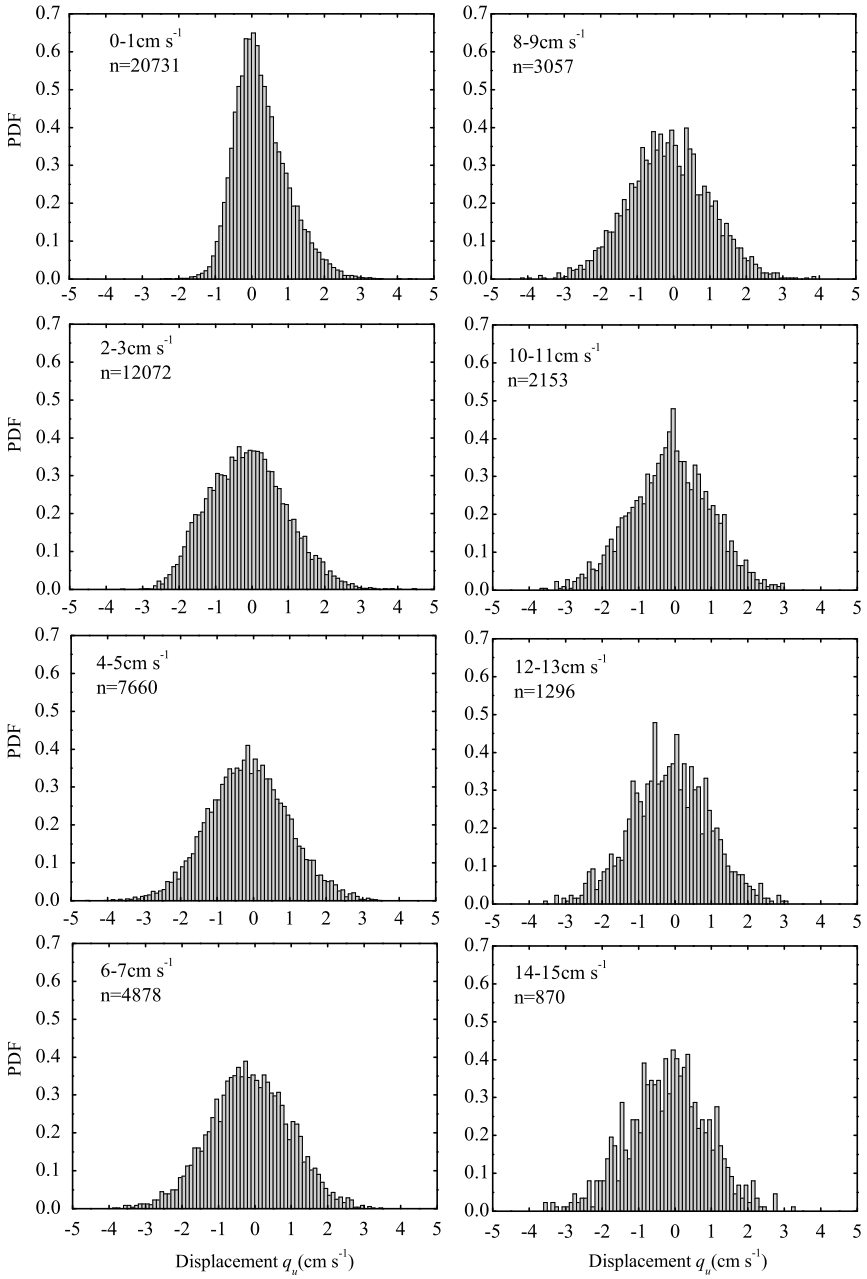

Figure 8. Histograms of the velocity displacements $q_u = u_p(t + \Delta t) - u_p(t)$ calculated from simulated particle motions and conditioned on the particle velocity u_p, varying in the indicated range for each panel (*n* indicates the number of data points used to compute each histogram). See Figure 6 in *Furbish et al.* [2012a] for comparison, but note the different *x* axis range.

flow depth), and their signature on the particle forces cannot be correctly described by a simple Gaussian white noise model of constant variance. The reason for the discussed discrepancies of the velocity displacement statistics for large particle velocities is thus intrinsically related to the simplification introduced in our stochastic model versus the complex vertical structure of the rough wall turbulent boundary layer. We note that the variance of the stochastic term in the random walk model of *Furbish et al.* [2012a] was selected to vary linearly with the square of the particle velocity, a parameterization directly suggested by the experimental data and indicating a coupling (via the local particle velocity) of the advective and diffusive momentum forces, in both the streamwise and cross-stream directions. It is no doubt that our model misses some details of this force coupling and further work should address this shortcoming. Ultimately, all these aspects need to be studied in a Lagrangian frame of reference in order to capture the physical mechanisms

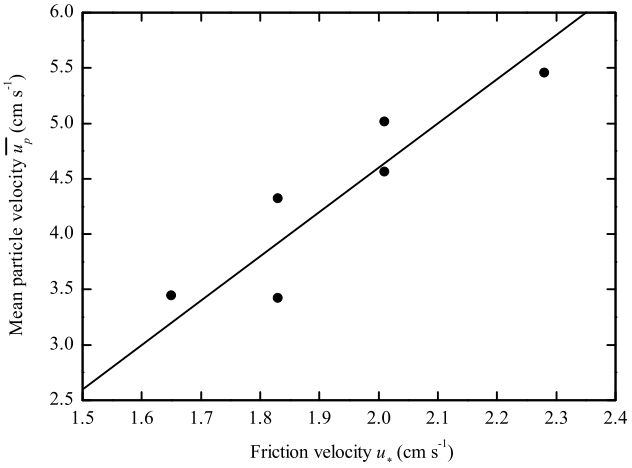

Figure 9. Plot of bed friction velocity u_* versus associated mean particle velocity $\overline{u_p}$ from the experiments conducted by *Roseberry et al.* [2012], which shows the linear relation $\overline{u_p} \propto u_*$ (solid line). Specifically the fitted relationship is $\overline{u_p} = 4.0(u_* - 0.55u_{*_c})$.

responsible for entrainment and disentrainment along the particle trajectories and better interpret the conditioned statistics on particle velocity.

4.2. Further Analysis of the Parameters

There are three parameters in our model describing the streamwise motion for particles: Δ_x, F_x, and D_x. Among them Δ_x is explicit as discussed in sections 3.2 and 4.1; F_x, which is the average downstream force, must be smaller than Δ_x, or the model will be invalid mathematically. This limitation can be understood since our model is only applicable for low transport rate conditions. Under such conditions, the particles' velocity will increase as the bed stress increases and, as a result, the relative velocity between the particles and the neighboring fluid will decrease together with the drag force. These analyses are consistent with previous studies by *Dominic* [1983] and *Bridge and Dominic* [1984].

D_x denotes the amplitude of the fluctuating force, a new parameter introduced by our model, which requires further study. Below, we demonstrate that D_x relates linearly to the bed friction velocity u_*. Given equation (15), multiplying u_p, and integrating with respect to u_p, we obtain the average of u_p:

$$\overline{u_p} = \int_{-\infty}^{+\infty} u_p \frac{\Delta_x^2 - F_x^2}{2\Delta_x D_x} \exp\left(\frac{-\Delta_x |u_p| + F_x u_p}{D_x}\right) du_p = \frac{2F_x D_x}{\Delta_x^2 - F_x^2} \tag{18}$$

Equation (18) indicates $\overline{u_p} \propto D_x$. Six runs of the experimental data set from *Roseberry et al.* [2012] confirm the linear relationship between $\overline{u_p}$ and the bed friction velocity u_* (Figure 9). From a linear regression we obtained the formula below:

$$\overline{u_p} = 4.0(u_* - 0.55u_{*c}) \tag{19}$$

where u_{*c} is the critical bed friction velocity calculated from the critical Shields number $\tau_{*c} = 0.03$ [*Shields*, 1936]. The linear relationship between $\overline{u_p}$ and u_* is consistent with the result by *Roseberry et al.* [2012], using the same data, who proposed the relation $\overline{u_p} \sim \sqrt{\tau_*}$. The data in Figure 9 are a bit scattered due to the limited number of experimental data (only six runs, with the duration of the experiments varying from 0.4 s to 19.6 s). However, the trend is clear. Apart from the results from the experimental data we used in this study, many studies have presented the relation $\overline{u_p} = a(u_* - bu_{*c})$ (where a and b are coefficients) derived experimentally [e.g., *Fernandez-Luque and Van Beek*, 1976; *Abbott and Francis*, 1977; *Niño et al.*, 1994; *Meier*, 1995; *Hu and Hui*, 1996] or theoretically [e.g., *Bridge and Dominic*, 1984; *Wiberg and Smith*, 1989]. A comprehensive review by *Lajeunesse et al.* [2010] suggested that the coefficient a was in the range of 4.4 ~ 5.6 for an erodible bed, while our result indicates a value a little smaller than this range.

As a result of this, we have $D_x \propto u_*$. Since D_x has the dimension $[L^2 \cdot T^{-3}]$, we can propose the relation $D_x \propto u_* g$. From the Reynolds stress intensity close to the wall boundary for turbulent open channel flows [*Nezu and Nakagawa*, 1993; *Nezu and Sanjou*, 2011], u_* is derived and can be used as a scale for turbulence intensity near the bed [*Nezu and Rodi*, 1986]. Following the above consideration and recalling the Townsend similarity on rough wall boundary layers [*Flack et al.* 2005], the new parameter D_x in our model can be interpreted as a measure of the turbulence intensity near the bed surface and may possibly be derived independently.

Previous studies have shown that fluctuating forces play an important role in sediment transport [e.g., *Schmeeckle and Nelson*, 2003; *Sumer et al.*, 2003; *Cheng et al.*, 2004; *Schmeeckle et al.*, 2007; *Valyrakis et al.*, 2010; *Tregnaghi et al.*, 2012b]. For example, *Sumer et al.* [2003] experimentally showed that the transport rate can

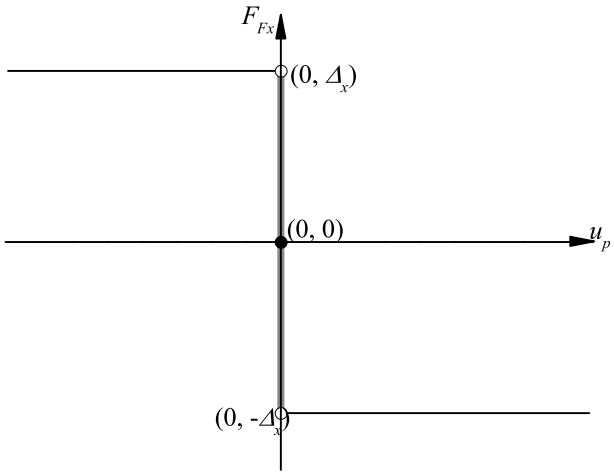

Figure 10. Sketch of the singularity of the friction force F_{Fx}. The convention sign(0) = 0 introduces a discontinuity of F_{Fx} at the point $u_p = 0$; however, this point is not only discontinuous but also multivalued as F_{Fx} can range from $-\Delta_x$ to Δ_x (the gray thick line).

vary up to 50 times without changes in the average bed shear stress, only by altering the turbulence fluctuations, especially under low transport rate conditions. *Schmeeckle et al*. [2007] noted that the fluctuating forces were responsible for entraining and moving the particles, rather than any average characteristic of the flow. Our study indicates that particles can move even when the average downstream force is less than the resistant force, namely, $\Delta_x = 3.66\ \mathrm{m \cdot s^{-2}}$ and $F_x = 3.17\ \mathrm{m \cdot s^{-2}}$, which stresses the importance of stochastic forces in sediment transport.

4.3. Singularity of the Model

For this study, the point where the particle velocity is zero is a singular point. As the Coulomb-like friction is adopted, we use the sign function sign(·) and adopt the convention of sign(0) = 0. This convention was also used in the fields of theoretical physics by *de Gennes* [2005] and *Touchette et al*. [2010] and granular materials by *Kawarada and Hayakawa* [2004]. As shown in Figure 10, the friction force F_{Fx} is discontinuous at the point $u_p = 0$. The FPE is however considered to be valid, even though the discontinuous point exists [*Kawarada and Hayakawa*, 2004; *Touchette et al*., 2010]. The numerical simulation of the LE in this study confirms that the FPE is applicable (Figure 5), and the discontinuity produces a cusp singular point in the PDF given by the FPE. The mathematical proof is beyond the scope of this study.

In principle, the point $u_p = 0$ is not only discontinuous but also multivalued, as the friction force F_{Fx} can range from $-\Delta_x$ to Δ_x. As a result, when the magnitude of the particle velocity falls to zero, the particle will stop for a while, rather than move immediately; this phenomenon is called "stick slip" in the field of theoretical physics [e.g., *Heslot et al*., 1994; *Urbakh et al*., 2004; *Touchette et al*., 2012]. However, in our study, as well as in the models by *Kawarada and Hayakawa* [2004] and *Touchette et al*. [2010], the convention of sign(0) = 0 (single valued) is adopted, that is, we remove the singularity from the function but preserve it in its derivative. This implies that the simulated particles are always in motion (Figure 4), and the stick-slip phenomenon, i.e., that once a particle disentrains, it might wait for a while to entrain again [*Valyrakis et al*., 2011; *Heyman et al*., 2013], cannot be reproduced in our model. In a future study we will incorporate waiting times in our proposed model to simulate stick-slip behavior and explore its effect on the characteristics of bed load transport.

5. Conclusions

In this paper we describe a hybrid mechanistic-stochastic model for bed load transport under low transport rate conditions (i.e., rolling and sliding regimes). The model is inspired by the recent work reported in *Furbish et al*. [2012a, 2012b] and references therein. It comprises (1) the Langevin equations (LE) in the streamwise and cross-stream directions, which describe the evolution of velocities of individual particles as a function of the actual forces exerted on them, thus based on the microscale system properties, and (2) the Fokker-Planck equations (FPE) derived from the LEs, which express the PDF of velocities of the ensemble of particles, thus describing the macroscale statistical properties of the system. The derivation of the FPE from the mechanistically formulated LE, representing a key contribution in this work, provides in fact a physically based connection between the statistical description of sediment transport and the fluctuating forces exerted on individual particles associated with the unsteady component of drag and friction due to turbulence and particle bed interactions.

Our study indicates that the exponential-like PDFs of particle velocities which have been reported from experimental studies for bed load particles under quasi-steady conditions [*Roseberry et al*., 2012] result

theoretically from the forces exerted on the individual particles, specifically from the friction force F_{Fx}, the average downstream force F_x, and the stochastic component ξ_x, assumed Gaussian white noise with variance D_x.

In addition to the particle velocity distribution, the simulated trajectories obtained from the LE allow us to quantify the hop distance λ and travel time τ and to satisfactorily compare their relationship with the experimental data, confirming the nonlinear dependency $\lambda \propto \tau^{5/3}$ and suggesting a correct representation of the micro scale properties of the system.

Our model also allows particles to move even when the average downstream force is less than the resistance force, which stresses the importance of stochastic forces in sediment transport [e.g., *Schmeeckle et al.*, 2007]. This is emphasized by the parameter D_x, which is dimensionally expressed as $D_x \propto u_* g$, and thus related to turbulence intensities near the bed surface. While the stochastic component of the model correctly describes most of the mechanisms occurring at the particle scale (especially at the wall as implied in $D_x \propto u_* g$), it however fails to reproduce some phenomena observed in the experiments, such as the stick-slip phenomenon of particle motions [*Heyman et al.*, 2013] and the strong tails in the distribution of particle acceleration for relatively large particle velocities [*Furbish et al.*, 2012a]. We suggest that these limitations can be attributed to the strong coherence of turbulent structures (above the roughness sublayer), which cannot be included in our stochastic model. We hope to extend our analysis in future work to other aspects of bed load transport, e.g., particle dispersion and multiscale properties.

Appendix A: Langevin and Fokker-Planck Equations

The derivation presented here is a simplified form of the derivation presented in *Risken* [1989].

The Langevin equation for particle streamwise velocity is

$$\frac{\mathrm{d}u_p}{\mathrm{d}t} = f(u_p) + \xi(t) \tag{A1}$$

The Langevin force $\xi(t)$ is Gaussian white noise

$$\begin{aligned} \langle \xi(t) \rangle &= 0 \\ \langle \xi(t_1)\xi(t_2) \rangle &= 2D_x \delta(t_2 - t_1) \\ \langle \xi(t_1)\xi(t_2)\cdots\xi(t_{2n-1}) \rangle &= 0 \\ \langle \xi(t_1)\xi(t_2)\cdots\xi(t_{2n}) \rangle &= (2D_x)^n \Sigma[\delta(t_{i_1} - t_{i_2})\cdots\delta(t_{i_{2n-1}} - t_{i_{2n}})] \end{aligned} \tag{A2}$$

where δ is the Dirac delta function, which refers to the "white" property of the noise.

When $f(u_p)$ is nonlinear, it is difficult to solve (A1) directly, so we focus on the evolution of the probability density function of x: $\rho_{u_p}(u_p, t)$. The partial derivative $\rho_{u_p}(u_p, t)$ with respect to t satisfies

$$\frac{\partial \rho_{u_p}(u_p, t)}{\partial t} = \lim_{\Delta \mathrm{t} \to 0} \frac{\rho_{u_p}(u_p, t + \Delta \mathrm{t}) - \rho_{u_p}(u_p, t)}{\Delta \mathrm{t}} \tag{A3}$$

The process $u_p(t)$ is a Markov process, so we have the Chapman-Kolmogorov equation

$$\rho_{u_p}(u_p, t + \Delta t) = \int_{-\infty}^{+\infty} p\left(u_p, t + \Delta t \middle| u_p', t\right) \rho_{u_p}\left(u_p', t\right) du_p' \tag{A4}$$

where $p\left(u_p, t + \Delta t \middle| u_p', t\right)$ is the transition probability between t and $t + \Delta t$.

According to the property of the Dirac delta function, we have

$$p\left(u_p, t + \Delta t \middle| u_p', t\right) = \int_{-\infty}^{+\infty} \delta(y - u_p) p\left(y, t + \Delta t \middle| u_p', t\right) dy \tag{A5}$$

By expanding the Dirac delta function as a Taylor series, we get

$$\delta(y-u_p)=\delta\left(y-u_p'+u_p'-u_p\right)=\sum_{n=0}^{\infty}\frac{\left(y-u_p'\right)^2}{n!}\left(\frac{\partial}{\partial u_p'}\right)\delta\left(u_p'-u_p\right)$$
$$=\sum_{n=0}^{\infty}\frac{\left(y-u_p'\right)^2}{n!}\left(-\frac{\partial}{\partial u_p}\right)^n\delta\left(u_p'-u_p\right) \tag{A6}$$

Substituting (A6) into (A5) gives

$$p\left(u_p,t+\Delta t\middle|u_p',t\right)=\sum_{n=0}^{\infty}\frac{1}{n!}\left(-\frac{\partial}{\partial u_p}\right)^2\left(\int_{-\infty}^{+\infty}\left(u_p-u_p'\right)^n p\left(y,t+\Delta t\middle|u_p',t\right)dy\right)\delta\left(u_p'-u_p\right) \tag{A7}$$

Let $M_n\left(u_p',t,\Delta t\right)$ denote the nth moment centered at the initial value x', which satisfies

$$M_n\left(u_p',t,\Delta t\right)^n=\int_{-\infty}^{+\infty}\delta\left(y-u_p'\right)^n p\left(y,t+\Delta t\middle|u_p',t\right)dy=\left\langle u_p'(t+\Delta t)-u_p'(t)\right\rangle^n \tag{A8}$$

The $\langle\cdot\rangle$ denotes average, so we rewrite (A7) as

$$p\left(u_p,t+\Delta t\middle|u_p',t\right)=\left[1+\sum_{n=1}^{\infty}\frac{1}{n!}\left(-\frac{\partial}{\partial u_p}\right)^n M_n\left(u_p',t,\Delta t\right)\right]\delta\left(u_p'-u_p\right)$$
$$=\left[1+\sum_{n=1}^{\infty}\frac{1}{n!}\left(-\frac{\partial}{\partial u_p}\right)^n M_n\left(u_p,t,\Delta t\right)\right]\delta\left(u_p-u_p'\right) \tag{A9}$$

Substituting (A4) and (A9) into (A3) gives

$$\frac{\partial\rho_{u_p}\left(u_p,t\right)}{\partial t}=\lim_{\Delta t\to 0}\frac{\rho_{u_p}\left(u_p,t+\Delta t\right)-\rho_{u_p}\left(u_p,t\right)}{\Delta t}$$
$$=\left\{\sum_{n=1}^{\infty}\left(-\frac{\partial}{\partial u_p}\right)^n D_n\left(u_p,t\right)^n\right\}\rho_{u_p}\left(u_p,t\right) \tag{A10}$$

where the Kramers-Moyal coefficients $D_n(u_p,\ t)$ are defined as

$$D_n\left(u_p,t\right)=\lim_{\Delta t\to 0}\frac{M_n\left(u_p,t,\Delta t\right)}{n!\Delta t} \tag{A11}$$

(A10) and (A11) are Kramers-Moyal Expansion for Markov process.

To derive these Kramers-Moyal coefficients, we first write the Langevin equation (A1) in the form of an integral equation

$$u_p(t+\Delta t)-u_p(t)=\int_t^{t+\Delta t}\left[f\left(u_p\left(t'\right)\right)+\xi\left(t'\right)\right]dt' \tag{A12}$$

Then, assuming that f can be expanded as a Taylor series

$$f\left(u_p\left(t'\right)\right)=f\left(u_p\right)+f'\left(u_p\right)\left[u_p\left(t'\right)-u_p\right]+\frac{1}{2}f''\left(u_p\right)\left[u_p\left(t'\right)-u_p\right]^2+\cdots \tag{A13}$$

Respectively, f' and f'' denote the first- and second-order derivates with respect to x. Inserting (A13) into (A12) leads to

$$u_p(t+\Delta t)-u_p(t)=\int_t^{t+\Delta t} f(u_p)dt'+\int_t^{t+\Delta t} f'(u_p)\left[u_p(t')-u_p\right]dt' + \frac{1}{2}\int_t^{t+\Delta t} f''(u_p)\left[u_p(t')-u_p\right]^2 dt'+\cdots+\int_t^{t+\Delta t}\xi(t')dt' \tag{A14}$$

For $u_p(t')-u_p$ in the integrand, we iterate (A13), producing

$$u_p(t+\Delta t)-u_p(t)=\int_t^{t+\Delta t} f(u_p)dt'+\int_t^{t+\Delta t} f'(u_p)\int_t^{t'} f(u_p)dt''dt'+\int_t^{t+\Delta t} f'(u_p)\int_t^{t'}\xi(t'')dt''dt'+\cdots+\int_t^{t+\Delta t}\xi(t')dt' \tag{A15}$$

By repeated iterations of only Langevin forces, the known function f and its derivates appear on the right side of (A14).

From the property of the Langevin force as (A2), it follows that

$$\left\langle \int_t^{t+\Delta t}\cdots\xi(t_1)\int_t^{t_1}\cdots\xi(t_2)\int_t^{t_2}\cdots\xi(t_3)\cdots\int_t^{t_{2n-2}}\cdots\xi(t_{2n-1})dt_1dt_2\cdots dt_m\right\rangle=0 \tag{A16}$$

$$\left\langle \int_t^{t+\Delta t}\cdots\xi(t_1)\int_t^{t_1}\cdots\xi(t_2)\int_t^{t_2}\cdots\xi(t_3)\cdots\int_t^{t_{2n-2}}\cdots\xi(t_{2n})dt_1dt_2\cdots dt_m\right\rangle=o(\Delta t^{m-n}) \tag{A17}$$

Both m and n are positive integers and assuming $m \geq n$. So if we now take the average of (A15), and using the agreements as (A16) and (A17), most components vanish, and we obtain

$$\begin{aligned} M_1(u_p,t,\Delta t) &= \langle u_p(t+\Delta t)-u_p(t)\rangle \\ &= \left\langle \int_t^{t+\Delta t} f(u_p)dt'+\int_t^{t+\Delta t} f'(u_p)\int_t^{t+\Delta t} f(u_p)dt''dt'+\cdots\right\rangle \\ &= f\left(u_p\right)\Delta t+o(\Delta t^2) \end{aligned} \tag{A18}$$

Then we get the first-order Kramers-Moyal coefficient

$$D_1(u_p,t)=f(u_p) \tag{A19}$$

and similarly

$$M_2(u_p,t,\Delta t)=\left\langle\left(u_p(t+\Delta t)-u_p(t)\right)^2\right\rangle=\left\langle\int_t^{t+\Delta t}\int_t^{t+\Delta t} 2\delta(t'-t'')dt'dt''+\cdots\right\rangle=2D_x\Delta t+o(\Delta t^2) \tag{A20}$$

For the second-order Kramers-Moyal coefficient

$$D_2(u_p,t)=D_x \tag{A21}$$

For $n \geq 3$, all Kramers-Moyal coefficients vanish. So we obtain the Fokker-Planck equation

$$\frac{\partial\rho_{u_p}(u_p,t)}{\partial t}=-\frac{\partial}{\partial u_p}\left[f(u_p)\rho_{u_p}(u_p,t)\right]+D_x\frac{\partial^2\rho_{u_p}(u_p,t)}{\partial u_p^2} \tag{A22}$$

Here $f(u_p)=-\Delta_x\cdot\mathrm{sign}(u_p)+F_x$, so equation (A22) turns into

$$\frac{\partial\rho_{u_p}}{\partial t}=-\frac{\partial}{\partial u_p}\left\{\left[F_x-\Delta_x\cdot\mathrm{sign}(u_p)\right]\rho_{u_p}\right\}+D_x\frac{\partial^2\rho_{u_p}}{\partial u_p^2} \tag{A23}$$

Notation

A_f area of the particle exposed to the fluid [L^2].
a, b linear regression coefficients for mean particle velocity (see equation (19)).
a_x acceleration in the streamwise direction [$L \cdot T^{-2}$].
C normalization constant for the PDF [$L^{-1} \cdot T$] (see equation (13)).
C_D drag coefficient.
D_n nth-order Kramers-Moyal coefficients (see equation (A11)).
D_x, D_y parameters denoting the amplitude of fluctuating force in streamwise and cross-stream directions [$L^2 \cdot T^{-3}$] (see equation (6)).
d particle diameter [L].
F_{Accx} the acceleration force of a particle per unit mass [$L \cdot T^{-2}$].
F_{Dx} actual force exerted by the fluid on a particle per unit mass in streamwise direction [$L \cdot T^{-2}$].
F_{Fx}, F_{Fx} friction force exerted on a particle per unit mass in streamwise and cross-stream direction [$L \cdot T^{-2}$].
F_r Froude number.
F_x mean downstream force exerted on a particle per unit mass [$L \cdot T^{-2}$].
F_1, F_2 Runge-Kutta coefficients.
g gravitational acceleration [$L \cdot T^{-2}$] .
M_n nth moment centered at the initial value.
p the transition probability.
Re_* particle Reynolds number in which $Re_* = u_* d/\upsilon$
t time [T]
t_s period for an ensemble of particle to reach the steady state condition starting from zero velocity by equation (17) [T].
u_f fluid velocity [$L \cdot T^{-1}$].
u_p, v_p velocity of a particle in streamwise and cross-stream directions [$L \cdot T^{-1}$].
u_r relative velocity between particle and fluid in streamwise direction [$L \cdot T^{-1}$].
u_* bed friction velocity [$L \cdot T^{-1}$].
u_{*_c} critical bed friction velocity [$L \cdot T^{-1}$].
v_r relative velocity between particle and fluid in cross-stream direction [$L \cdot T^{-1}$].
W submerged weight of a particle per unit mass [$L \cdot T^{-2}$].
w_0, w_1 w_2 three independent standard Gaussian distribution random numbers.
w_r relative velocity between particle and fluid in the vertical direction [$L \cdot T^{-1}$].
Δ_x, Δy shorthand expressions for friction force in streamwise and cross-stream directions [$L \cdot T^{-2}$] (see equation (2)).
δ Dirac delta function.
λ hop distance of a particle [L].
μ dynamic friction coefficient.
o order of the magnitude of the variable.
θ slope of bed.
ρ_f, ρ_p density of fluid and particle [$M \cdot L^{-3}$].
ρ_{u_p}, ρ_{v_p} PDF of the particle streamwise and cross-stream velocities [$L^{-1} \cdot T$].
τ travel time of a particle [T]
τ_* dimensionless bed stress or Shields number [1].
τ_{*_c} critical dimensionless bed stress [1].
ξ_x, ξ_y Gaussian white noise in streamwise and cross-stream directions [$L \cdot T^{-2}$] (see equations (5) and (7)).

Acknowledgments
We would like to thank the group of David Jon Furbish who provided us with the experimental data. The Editor Alexander Densmore, Associate Editor Wonsuck Kim, and three reviewers (Brandon McElroy, Phairot Chatanantavet, and an anonymous reviewer) provided constructive comments that considerably improved the presentation of our work. We are also grateful to David Jon Furbish and Kimberly Hill for insightful discussions, and Arvind Singh and Leonardo Chamorro for reviewing earlier versions of this paper. Financial support from the National Natural Science Foundation of China (grant 51039004), National Science and Technology Supporting Plan of the Twelfth Five-year (grant 2012BAB02B02) and support from the National Center for Earth-Surface Dynamics (NCED), funded under NSF grant EAR-0120914, and an NSF Water Sustainability and Climate project (grant CBET-1209402) are gratefully acknowledged. Niannian Fan received a fellowship from the China Scholarship Council for his visit to the University of Minnesota.

References

Abbott, J., and J. Francis (1977), Saltation and suspension trajectories of solid grains in a water stream, *Philos. Trans. R. Soc. London A*, *284*, 225–254.

Abrahams, A. D. (2003), Bed-load transport equation for sheet flow, *J. Hydraul. Eng.-ASCE*, *129*(2), 159–163, doi:10.1061/(ASCE)0733-9429(2003)129:2(159).

Abrahams, A. D., and P. Gao (2006), A bed-load transport model for rough turbulent open-channel flows on plane beds, *Earth Surf. Process. Landforms.*, *31*(7), 910–928, doi:10.1002/esp.1300.

Ancey, C. (2010), Stochastic modeling in sediment dynamics: Exner equation for planar bed incipient bed load transport conditions, *J. Geophys. Res.*, *115*, F00A11, doi:10.1029/2009JF001260.
Ancey, C., F. Bigillon, P. Frey, and R. Ducret (2003), Rolling motion of a bead in a rapid water stream, *Phys. Rev. E*, *67*, (01130311).
Ancey, C., T. Böhm, M. Jodeau, and P. Frey (2006), Statistical description of sediment transport experiments, *Phys. Rev. E*, *74*(011302), doi:10.1103/PhysRevE.74.011302.
Ancey, C., A. C. Davison, T. Böhm, M. Jodeau, and P. Frey (2008), Entrainment and motion of coarse particles in a shallow water stream down a steep slope, *J. Fluid Mech.*, *595*, 83–114, doi:10.1017/S0022112007008774.
Bagnold, R. A. (1966), An approach to the sediment transport problem from general physics, *U.S. Geol. Surv. Prof. Pap.*, *4221*, 1–37.
Bagnold, R. A. (1973), The nature of saltation and of 'bed-load' transport in water, *Proc. R. Soc. London, Ser. A*, *332*, 473–504.
Bagnold, R. A. (1977), Bed load transport by natural rivers, *Water Resour. Res.*, *13*(2), 303–312.
Batrouni, G. G., S. Dippel, and L. Samson (1996), Stochastic model for the motion of a particle on an inclined rough plane and the onset of viscous friction, *Phys. Rev. E*, *53*(6), 6496–6503.
Baule, A., and P. Sollich (2012), Singular features in noise-induced transport with dry friction, *EPL*, *97*(200012), doi:10.1209/0295-5075/97/20001.
Best, J. (2005), The fluid dynamics of river dunes: A review and some future research directions, *J. Geophys. Res.*, *110*, F04S02F4, doi:10.1029/2004JF000218.
Bradley, D. N., G. E. Tucker, and D. A. Benson (2010), Fractional dispersion in a sand bed river, *J. Geophys. Res.*, *115*, F00A09, doi:10.1029/2009JF001268.
Bridge, J. S., and S. J. Bennett (1992), A model for the entrainment and transport of sediment grains of mixed sizes, shapes, and densities, *Water Resour. Res.*, *28*(2), 337–363.
Bridge, J. S., and D. F. Dominic (1984), Bed load grain velocities and sediment transport rates, *Water Resour. Res.*, *20*(4), 476–490.
Brouwers, J. J. H. (2010), Langevin and diffusion equation of turbulent fluid flow, *Phys. Fluids*, *22*(0851028).
Cheng, N. S., H. W. Tang, and L. J. Zhu (2004), Evaluation of bed load transport subject to high shear stress fluctuations, *Water Resour. Res.*, *40*, W056015, doi:10.1029/2003WR003001.
Chien, N., and Z. H. Wan (1998), *Mechanics of Sediment Transport*, ASCE Press, New York.
Church, M. (2006), Bed material transport and the morphology of alluvial river channels, *Annu. Rev. Earth Planet. Sci.*, *34*, 325–354, doi:10.1146/annurev.earth.33.092203.122721.
de Gennes, P. G. (2005), Brownian motion with dry friction, *J. Stat. Phys.*, *119*(5-6), 953–962, doi:10.1007/s10955-005-4650-4.
Diplas, P., C. L. Dancey, A. O. Celik, M. Valyrakis, K. Greer, and T. Akar (2008), The role of impulse on the initiation of particle movement under turbulent flow conditions, *Science*, *322*(5902), 717–720, doi:10.1126/science.1158954.
Diplas, P., A. O. Celik, C. L. Dancey, and M. Valyrakis (2010), Nonintrusive method for detecting particle movement characteristics near threshold flow conditions, *J. Irrig. Drain. E.*, *136*(11), 774–780, doi:10.1061/(ASCE)IR.1943-4774.0000252.
Dominic, D. F. (1983), *Evaluation of Bedload Sediment Transport Models*, Master's thesis, State Univ. of N.Y, Binghamton.
Drake, T. G., R. L. Shreve, W. E. Dietrich, P. J. Whiting, and L. B. Leopold (1988), Bedload transport of fine gravel observed by motion-picture photography, *J. Fluid Mech.*, *192*, 193–217.
Einstein, H. A. (1937), Der Geschiebetrieb als Wahrscheinlichkeitsproblem, in *Mitteilung der Versuchsanstalt für Wasserbau an der Eidgenössische Technische Hochschule Zürich*, Rascher, Zurich, Switzerland, English translation, Sedimentation, edited by H. W. Shen, pp. C1–C105, Colo. State Univ., Fort Collins.
Einstein, H. A. (1950), *The Bed-Load Function for Sediment Transportation in Open Channel Flows*, Technical Bulletin, vol. 1026, pp. 78, Soil Conserv. Serv., U.S. Dep. of Agric., Washington, D. C.
Fernandez-Luque, R., and R. Van Beek (1976), Erosion and transport of bed-load sediment, *J. Hydraul. Res.*, *14*, 127–144.
Flack, K. A., M. P. Schultz, and T. A. Shapiro (2005), Experimental support for Townsend's Reynolds number similarity hypothesis on rough walls, *Phys. Fluids*, *17*, (0351023), doi:10.1063/1.1843135
Foufoula-Georgiou, E., and C. Stark (2010), Introduction to special section on Stochastic Transport and Emergent Scaling on Earth's Surface: Rethinking geomorphic transport—Stochastic theories, broad scales of motion and nonlocality, *J. Geophys. Res.*, *115*, F00A01, doi:10.1029/2010JF001661.
Francalanci, S., and L. Solari (2007), Gravitational effects on bed load transport at low Shields stress: Experimental observations, *Water Resour. Res.*, *43*, W034243, doi:10.1029/2005WR004715.
Frey, P., and M. Church (2011), Bedload: A granular phenomenon, *Earth Surf. Process. Landforms.*, *36*(1), 58–69.
Furbish, D. J., and M. W. Schmeeckle (2013), A probabilistic derivation of the exponential-like distribution of bed load particle velocities, *Water Resour. Res.*, *49*, 1537–1551, doi:10.1002/wrcr.20074.
Furbish, D. J., J. C. Roseberry, and M. W. Schmeeckle (2012a), A probabilistic description of the bed load sediment flux: 3. The particle velocity distribution and the diffusive flux, *J. Geophys. Res.*, *117*, F03033, doi:10.1029/2012JF002355.
Furbish, D. J., P. K. Haff, J. C. Roseberry, and M. W. Schmeeckle (2012b), A probabilistic description of the bed load sediment flux: 1. Theory, *J. Geophys. Res.*, *117*, F03031, doi:10.1029/2012JF002352.
Furbish, D. J., A. E. Ball, and M. W. Schmeeckle (2012c), A probabilistic description of the bed load sediment flux: 4. Fickian diffusion at low transport rates, *J. Geophys. Res.*, *117*, F03034, doi:10.1029/2012JF002356.
Gabet, E. J., and M. K. Mendoza (2012), Particle transport over rough hillslope surfaces by dry ravel: Experiments and simulations with implications for nonlocal sediment flux, *J. Geophys. Res.*, *117*, F01019, doi:10.1029/2011JF002229.
Ganti, V., M. M. Meerschaert, E. Foufoula-Georgiou, E. Viparelli, and G. Parker (2010), Normal and anomalous diffusion of gravel tracer particles in rivers, *J. Geophys. Res.*, *115*, F00A12, doi:10.1029/2008JF001222.
Gao, P. (2008), Transition between two bed-load transport regimes: Saltation and sheet flow, *J. Hydraul. Eng.-ASCE*, *134*(3), 340–349, doi:10.1061/(ASCE)0733-9429(2008)134:3(340).
Gardiner, C. W. (1983), *Handbook of Stochastic Methods*, Springer, Berlin.
Guala, M., S. E. Hommema, and R. J. Adrian (2006), Large-scale and very-large-scale motions in turbulent pipe flow, *J. Fluid Mech.*, *554*, 521–542, doi:10.1017/S0022112006008871.
Guala, M., M. Metzger, and B. J. McKeon (2011), Interactions within the turbulent boundary layer at high Reynolds number, *J. Fluid Mech.*, *666*, 573–604, doi:10.1017/S0022112010004544.
Hanes, D. M. (1986), Grain flows and bed-load sediment transport: Review and extension, *Acta Mech.*, *63*(1-4), 131–142, doi:10.1007/BF01182544.
Hanes, D. M., and A. J. Bowen (1985), A granular-fluid model for steady intense bed-load transport, *J. Geophys. Res.*, *90*(NC5), 9149–9158.
Hassan, M. A., M. Church, and A. P. Schick (1991), Distance of movement of coarse particles in gravel bed streams, *Water Resour. Res.*, *27*(4), 503–511.
Hassan, M. A., H. Voepel, R. Schumer, G. Parker, and L. Fraccarollo (2013), Displacement characteristics of coarse fluvial bed sediment, *J. Geophys. Res. Earth Surface*, *118*, 155–165, doi:10.1029/2012JF002374.

Heslot, F., T. Baumberger, B. Perrin, B. Caroli, and C. Caroli (1994), Creep, stick-slip, and dry-friction dynamics: Experiments and a heuristic model, *Phys. Rev. E*, *49*(6Part a), 4973–4988, doi:10.1103/PhysRevE.49.4973.
Heyman, J., F. Mettra, H. Ma, and C. Ancey (2013), Statistics of bedload transport over steep slopes: Separation of time scales and collective motion, *Geophys. Res. Lett.*, *40*, 128–133, doi:10.1029/2012GL054280.
Hill, K. M., L. DellAngelo, and M. M. Meerschaert (2010), Heavy-tailed travel distance in gravel bed transport: An exploratory enquiry, *J. Geophys. Res.*, *115*, F00A14, doi:10.1029/2009JF001276.
Hofland, B., and J. A. Battjes (2006), Probability density function of instantaneous drag forces and shear stresses on a bed, *J. Hydraul. Eng.-ASCE*, *132*(11), 1169–1175, doi:10.1061/(ASCE)0733-9429(2006)132:11(1169).
Hofland, B., J. A. Battjes, and R. Booij (2005), Measurement of fluctuating pressures on coarse bed material, *J. Hydraul. Eng.-ASCE*, *131*(9), 770–781, doi:10.1061/(ASCE)0733-9429(2005)131:9(770).
Hu, C. H., and Q. C. Guo (2011), Near-bed sediment concentration distribution and basic probability of sediment movement, *J. Hydraul. Eng.-ASCE*, *137*(10), 1269–1275, doi:10.1061/(ASCE)HY.1943-7900.0000382.
Hu, C. H., and Y. J. Hui (1996), Bed-load transport. II: Stochastic characteristics, *J. Hydraul. Eng.-ASCE*, *122*(5), 255–261.
Hunt, A. G. (1999), A probabilistic treatment of fluvial entrainment of cohesionless particles, *J. Geophys. Res.*, *104*(B7), 15,409–15,413.
Jerolmack, D. J., and D. Mohrig (2005), A unified model for subaqueous bed form dynamics, *Water Resour. Res.*, *41*, W1242112, doi:10.1029/2005WR004329.
Kawarada, A., and H. Hayakawa (2004), Non-Gaussian velocity distribution function in a vibrating granular bed, *J. Phys. Soc. Jpn.*, *73*(8), 2037–2040, doi:10.1143/JPSJ.73.2037.
Keylock, C., A. Singh, and E. Foufoula-Georgiou (2013), The influence of migrating bedforms on the velocity-intermittency structure of turbulent flow over a gravel bed, *Geophys. Res. Lett.*, *40*, 1351–1355, doi:10.1002/grl.50337.
Lajeunesse, E., L. Malverti, and F. Charru (2010), Bed load transport in turbulent flow at the grain scale: Experiments and modeling, *J. Geophys. Res.*, *115*, F04001, doi:10.1029/2009JF001628.
Lee, H., and S. Balachandar (2012), Critical shear stress for incipient motion of a particle on a rough bed, *J. Geophys. Res.*, *117*, F01026, doi:10.1029/2011JF002208.
Liu, Y., F. Metivier, E. Lajeunesse, P. Lancien, C. Narteau, and P. Meunier (2008), Measuring bed load in gravel-bed mountain rivers: Averaging methods and sampling strategies, *Geodin. Acta*, *21*, 81–92.
Martin, R. L., D. J. Jerolmack, and R. Schumer (2012), The physical basis for anomalous diffusion in bed load transport, *J. Geophys. Res.*, *117*, F01018, doi:10.1029/2011JF002075.
Meier, C. I. (1995), Transport velocities of single bed-load grains in hydraulically smooth open channel flow, Master's thesis, Department of Civil Engineering, Colorado State University, Fort Collins, Colorado.
Métivier, F., P. Meunier, M. Moreira, A. Crave, C. Chaduteau, B. Ye, and G. Liu (2004), Transport dynamics and morphology of a high mountain stream during the peak flow season: The Ürümqi River (Chinese Tian Shan), in *River Flow 2004*, vol. 1, pp. 770–777, A. A. Balkema, Leiden, Netherlands.
Meunier, P., F. Métivier, E. Lajeunesse, A. S. Meriaux, and J. Faure (2006), Flow pattern and sediment transport in a braided river: The "torrent de St Pierre" (French Alps), *J. Hydrol.*, *330*, 496–505.
Minier, J. P., E. Peirano, and S. Chibbaro (2004), PDF model based on Langevin equation for polydispersed two-phase flows applied to a bluff-body gas-solid flow, *Phys. Fluids*, *16*(7), 2419–2431.
Monty, J. P., J. A. Stewart, R. C. Williams, and M. S. Chong (2007), Large-scale features in turbulent pipe and channel flows, *J. Fluid Mech.*, *589*, 147–156, doi:10.1017/S002211200700777X.
Murayama, Y., and M. Sano (1998), Transition from Gaussian to non-Gaussian velocity distribution functions in a vibrated granular bed, *J. Phys. Soc. Jpn.*, *67*(6), 1826–1829, doi:10.1143/JPSJ.67.1826.
Nezu, I., and H. Nakagawa (1993), *Turbulence in Open-Channel Flows*, Balkema, Rotterdam, The Netherlands.
Nezu, I., and W. Rodi (1986), Open-channel flow measurements with a laser Doppler anemometer, *J. Hydraul. Eng.-ASCE*, *112*(5), 335–355.
Nezu, I., and M. Sanjou (2011), PIV and PTV measurements in hydro-sciences with focus on turbulent open-channel flows, *J. Hydro-environ. Res.*, *5*(4SI), 215–230.
Nikora, V., H. Habersack, T. Huber, and I. McEwan (2002), On bed particle diffusion in gravel bed flows under weak bed load transport, *Water Resour. Res.*, *38*(6), 1081, doi:10.1029/2001WR000513.
Niño, Y., and M. García (1998a), Experiments on saltation of sand in water, *J. Hydraul. Eng.-ASCE*, *124*(10), 1014–1025.
Niño, Y., and M. García (1998b), Using Lagrangian particle saltation observations for bedload sediment transport modelling, *Hydrol. Process.*, *12*(8), 1197–1218.
Niño, Y., M. García, and L. Ayala (1994), Gravel saltation: 1. Experiments, *Water Resour. Res.*, *30*(6), 1907–1914.
Papanicolaou, A. N., P. Diplas, N. Evaggelopoulos, and S. Fotopoulos (2002), Stochastic incipient motion criterion for spheres under various bed packing conditions, *J. Hydraul. Eng.-ASCE*, *128*(4), 369–380, doi:10.1061/(ASCE)0733-9429(2002)128:4(369).
Parker, G., C. Paola, and S. Leclair (2000), Probabilistic Exner sediment continuity equation for mixtures with no active layer, *J. Hydraul. Eng.-ASCE*, *126*(11), 818-826, doi:10.1061/(ASCE)0733-9429(2000)126:11(818).
Parker, G., G. Seminara, and L. Solari (2003), Bed load at low Shields stress on arbitrarily sloping beds: Alternative entrainment formulation, *Water Resour. Res.*, *39*(7), 1183, doi:10.1029/2001WR001253.
Ramesh, B., U. C. Kothyari, and K. Murugesan (2011), Near-bed particle motion over transitionally-rough bed, *J. Hydraul. Res.*, *49*(6), 757–765, doi:10.1080/00221686.2011.620369.
Reynolds, A. M., and J. E. Cohen (2002), Stochastic simulation of heavy-particle trajectories in turbulent flows, *Phys. Fluids*, *14*(1), 342–351.
Risken, H. (1989), *The Fokker-Planck Equation: Methods of Solution and Applications*, 2nd ed., Springer, Berlin.
Roseberry, J. C., M. W. Schmeeckle, and D. J. Furbish (2012), A probabilistic description of the bed load sediment flux: 2. Particle activity and motions, *J. Geophys. Res.*, *117*, F03032, doi:10.1029/2012JF002353.
Schmeeckle, M. W., and J. M. Nelson (2003), Direct numerical simulation of bedload transport using a local, dynamic boundary condition, *Sedimentology*, *50*(2), 279–301, doi:10.1046/j.1365-3091.2003.00555.x.
Schmeeckle, M. W., J. M. Nelson, and R. L. Shreve (2007), Forces on stationary particles in near-bed turbulent flows, *J. Geophys. Res.*, *112*, F02003F2, doi:10.1029/2006JF000536.
Schmidt, K. H., and P. Ergenzinger (1992), Bedload entrainment, travel lengths, step lengths, rest periods—Studied with passive (iron, magnetic) and active (radio) tracer techniques, *Earth Surf. Process. Landforms.*, *17*(2), 147–165.
Seminara, G., L. Solari, and G. Parker (2002), Bed load at low Shields stress on arbitrarily sloping beds: Failure of the Bagnold hypothesis, *Water Resour. Res.*, *38*(11), 1249, doi:10.1029/2001WR000681.
Shields, I. (1936), Anwendung der Ahnlichkeitmechanik und der Turbulenz-Forschung auf die Gescheibebewegung, *Mitt. Preuss Vers. Wasserbau Schiffbau*, *26*, 5–24.

Singh, A., S. Lanzoni, and E. Foufoula-Georgiou (2009), Nonlinearity and complexity in gravel bed dynamics, *Stoch. Env. Res. Risk A.*, *23*(7), 967–975, doi:10.1007/s00477-008-0269-8.

Sumer, B. M., L. Chua, N. S. Cheng, and J. Fredsoe (2003), Influence of turbulence on bed load sediment transport, *J. Hydraul. Eng.-ASCE*, *129*(8), 585–596, doi:10.1061/(ASCE)0733-9429(2003)129:8(585).

Touchette, H., E. Van der Straeten, and W. Just (2010), Brownian motion with dry friction: Fokker-Planck approach, *J. Phys. A: Math. Theor.*, *43*(44500244), doi:10.1088/1751-8113/43/44/445002.

Touchette, H., T. Prellberg, and W. Just (2012), Exact power spectra of Brownian motion with solid friction, *J. Phys. A: Math. Theor.*, *45*(39500239), doi:10.1088/1751-8113/43/44/445002.

Tregnaghi, M., A. Bottacin-Busolin, A. Marion, and S. Tait (2012a), Stochastic determination of entrainment risk in uniformly sized sediment beds at low transport stages: 1. Theory, *J. Geophys. Res.*, *117*, F04004, doi:10.1029/2011JF002134.

Tregnaghi, M., A. Bottacin-Busolin, S. Tait, and A. Marion (2012b), Stochastic determination of entrainment risk in uniformly sized sediment beds at low transport stages: 2. Experiments, *J. Geophys. Res.*, *117*, F04005, doi:10.1029/2011JF002135.

Tsujimoto, T. (1978), Probabilistic model of the process of bed load transport and its application to mobile-bed problems, PhD thesis, Kyoto Univ., Kyoto, Japan.

Urbakh, M., J. Klafter, D. Gourdon, and J. Israelachvili (2004), The nonlinear nature of friction, *Nature*, *430*(6999), 525–528, doi:10.1038/nature02750.

Valyrakis, M., P. Diplas, C. L. Dancey, K. Greer, and A. O. Celik (2010), Role of instantaneous force magnitude and duration on particle entrainment, *J. Geophys. Res.*, *115*, F02006, doi:10.1029/2008JF001247.

Valyrakis, M., P. Diplas, and C. L. Dancey (2011), Entrainment of coarse grains in turbulent flows: An extreme value theory approach, *Water Resour. Res.*, *47*, W09512, doi:10.1029/2010WR010236.

Van Kampen, N. G. (2010), *Stochastic Processes in Physics and Chemistry*, 3rd ed., Elsevier, Amsterdam, Holland.

Van Rijn, L. (1984), Sediment transport, part I: Bed load transport, *J. Hydraul. Eng.-ASCE*, *110*, 1431–1456.

Wiberg, P. L., and J. D. Smith (1985), A theoretical model for saltating grains in water, *J. Geophys. Res.*, *90*(NC4), 7341–7354.

Wiberg, P. L., and J. D. Smith (1989), Model for calculating bed load transport of sediment, *J. Hydraul. Eng.-ASCE*, *115*(1), 101–123.

Wong, M., G. Parker, P. DeVries, T. M. Brown, and S. J. Burges (2007), Experiments on dispersion of tracer stones under lower-regime plane-bed equilibrium bed load transport, *Water Resour. Res.*, *43*, W034403, doi:10.1029/2006WR005172.

Yalin, M. (1977), *Mechanics of Sediment Transport*, Pergamon, New York.

Yeganeh-Bakhtiary, A., B. Shabani, H. Gotoh, and S. S. Y. Wang (2009), A three-dimensional distinct element model for bed-load transport, *J. Hydraul. Res.*, *47*(2), 203–212, doi:10.3826/jhr.2009.3168.

Zhang, T. R. (2007), *Statistical Mechanics and Applications* [in Chinese], Metallurgical industry Press, Beijing.

Zhong, D. Y., G. Q. Wang, and Q. C. Sun (2011), Transport equation for suspended sediment based on two-fluid model of solid/liquid two-phase flows, *J. Hydraul. Eng.-ASCE*, *137*(5), 530–542, doi:10.1061/(ASCE)HY.1943-7900.0000331.